2015

Albumin-associated free fatty acids induce macropinocytosis in podocytes

Jun-Jae Chung
Washington University School of Medicine in St. Louis

Tobias B. Huber
Washington University School of Medicine in St. Louis

Markus Gödel
Washington University School of Medicine in St. Louis

George Jarad
Washington University School of Medicine in St. Louis

Björn Hartleben
Washington University School of Medicine in St. Louis

See next page for additional authors

Authors

Jun-Jae Chung, Tobias B. Huber, Markus Gödel, George Jarad, Björn Hartleben, Christopher Kwoh, Alexander Keil, Aleksey Karpitskiy, Jiancheng Hu, Christine J. Huh, Marina Cella, Richard W. Gross, Jeffrey H. Miner, and Andrey S. Shaw

Albumin-associated free fatty acids induce macropinocytosis in podocytes

Jun-Jae Chung,[1] Tobias B. Huber,[1,2,3] Markus Gödel,[1] George Jarad,[4] Björn Hartleben,[1] Christopher Kwoh,[4] Alexander Keil,[1] Aleksey Karpitskiy,[1] Jiancheng Hu,[1] Christine J. Huh,[5] Marina Cella,[1] Richard W. Gross,[6] Jeffrey H. Miner,[4] and Andrey S. Shaw[1]

[1]Department of Pathology and Immunology, Washington University School of Medicine, St. Louis, Missouri, USA. [2]Renal Division, University Medical Center Freiburg, Freiburg, Germany. [3]BIOSS Centre for Biological Signalling Studies, Albert-Ludwigs-University Freiburg, Freiburg, Germany. [4]Department of Medicine, Renal Division, [5]Department of Developmental Biology, and [6]Department of Chemistry, Washington University School of Medicine, St. Louis, Missouri, USA.

Podocytes are specialized epithelial cells in the kidney glomerulus that play important structural and functional roles in maintaining the filtration barrier. Nephrotic syndrome results from a breakdown of the kidney filtration barrier and is associated with proteinuria, hyperlipidemia, and edema. Additionally, podocytes undergo changes in morphology and internalize plasma proteins in response to this disorder. Here, we used fluid-phase tracers in murine models and determined that podocytes actively internalize fluid from the plasma and that the rate of internalization is increased when the filtration barrier is disrupted. In cultured podocytes, the presence of free fatty acids (FFAs) associated with serum albumin stimulated macropinocytosis through a pathway that involves FFA receptors, the Gβ/Gγ complex, and RAC1. Moreover, mice with elevated levels of plasma FFAs as the result of a high-fat diet were more susceptible to Adriamycin-induced proteinuria than were animals on standard chow. Together, these results support a model in which podocytes sense the disruption of the filtration barrier via FFAs bound to albumin and respond by enhancing fluid-phase uptake. The response to FFAs may function in the development of nephrotic syndrome by amplifying the effects of proteinuria.

Introduction

The kidney glomerular filter functions to remove small molecular wastes from the blood without the loss of large plasma proteins into the urine. The filter is composed of 3 layers: fenestrated endothelial cells, the glomerular basement membrane (GBM), and epithelial cells known as podocytes (1). The GBM is thought to act as a size- and charge-selective filter or gel. On the outer aspect of the GBM, podocytes spread out across capillary loops and form a tight interdigitating network of membrane extensions known as foot processes. The space between adjacent foot processes is covered by a specialized cell junction complex that allows the passage of fluid and solutes.

The exact mechanism of glomerular filtration is not completely understood and has been the subject of modeling studies (2–5). All of these models predict that the size selectivity of the GBM is not 100% effective and is, to a certain degree, permeable to plasma proteins. In an average human, approximately 180 liters of blood is filtered by the kidney daily. Even if the GBM filtration barrier is 99.9% effective, as predicted by the modeling studies, the total volume of blood flow would still result in significant amounts of plasma proteins crossing the GBM (~9 grams of albumin and ~180 mg of IgG crossing the GBM every 24 hours). Since the slit diaphragm is considered impermeable to proteins the size of albumin or larger, we postulated that podocytes must have a mechanism to handle proteins that have crossed the GBM.

It was proposed over 40 years ago that podocytes internalize and remove proteins that cross the GBM (6, 7). Numerous studies using electron microscopy have shown increased numbers of protein-containing vesicles in podocytes under nephrotic conditions in which there is significant leakage of proteins across the GBM (8–18). Previously, we showed that expression of the neonatal Fc receptor, a transcytosis receptor for Ig and albumin, allows podocytes to handle these proteins by internalization and transcytosis (19).

Fluid-phase uptake in cells occurs through 2 distinct processes (20). Micropinocytosis is a nonspecific process that results in small vesicles of less than 0.1 μm in diameter and involves both coated and noncoated vesicles (21). A second, more specialized process called macropinocytosis only occurs in certain cell types. It involves the formation of large vesicles measuring 0.2–5 μm in diameter that form at sites of membrane ruffling (22). Macropinocytosis is clathrin independent, but requires actin, RAC1, and PI 3-kinase (PI3K). In certain cells like immature DCs and macrophages, macropinocytosis is a constitutive process (23, 24); in other cells, it is induced by extracellular stimuli, such as growth factors (25). Macropinocytosis allows for efficient internalization of extracellular fluids (up to 1 cell volume of fluid/hour), and because of the larger size of the vesicles, it is also more efficient for the uptake of large-sized molecules.

Here, we discovered that podocytes internalize fluid via macropinocytosis and that the rate can be increased by free fatty acids (FFAs) bound to albumin. Distinct from other known regulators of macropinocytosis, we found that lipid-binding GPCRs and Gβ/Gγ subunits regulate macropinocytosis in podocytes. Macropinocytosis may function to maintain the GBM by removing proteins that cross the GBM. In a proteinuric setting, however, this response

Authorship note: Jun-Jae Chung, Tobias B. Huber, and Markus Gödel contributed equally to this work.
Conflict of interest: The authors have declared that no conflict of interest exists.
Submitted: October 22, 2014; **Accepted:** March 19, 2015.
Reference information: *J Clin Invest*. 2015;125(6):2307–2316. doi:10.1172/JCI79641.

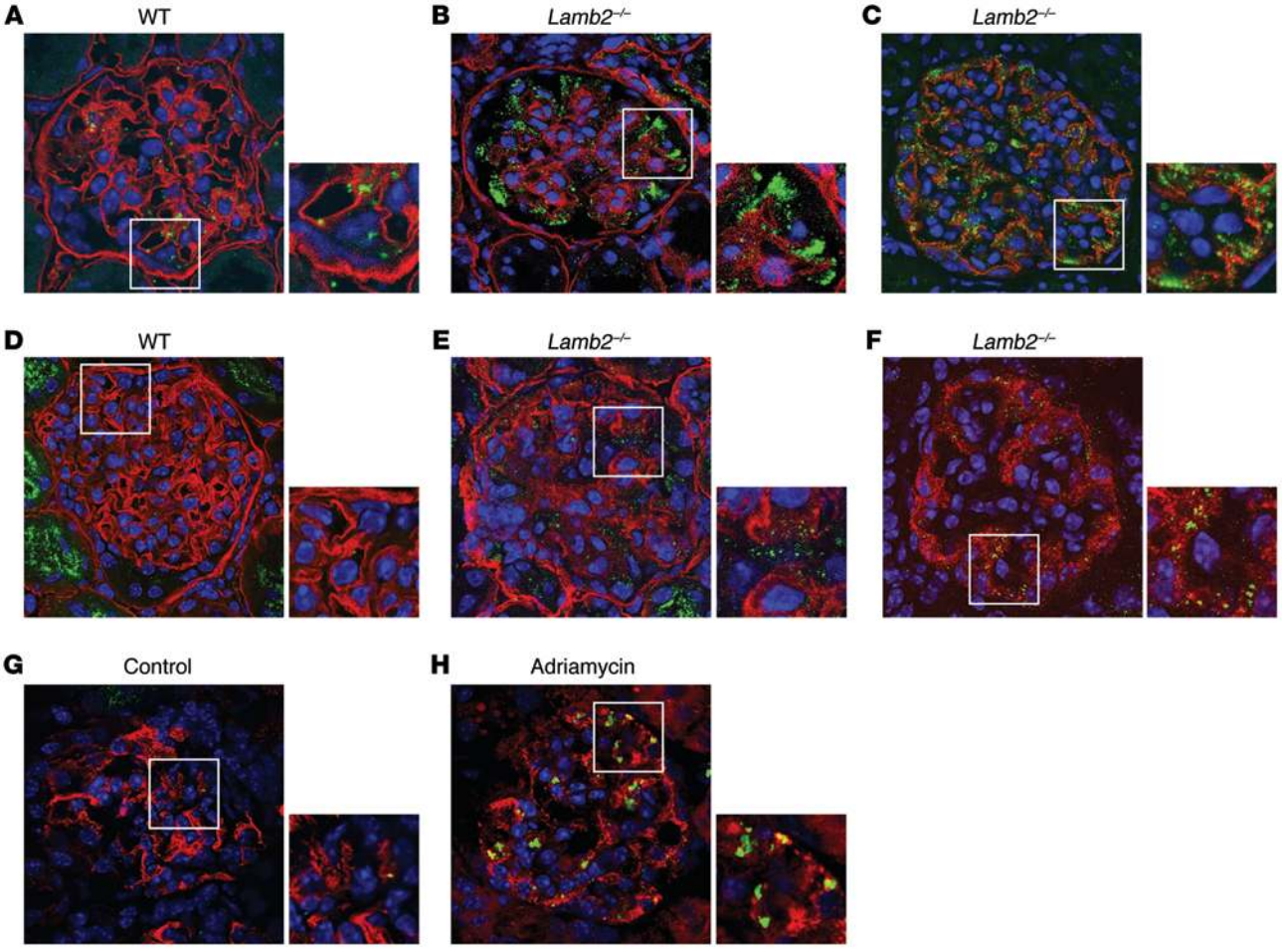

Figure 1. Podocytes are highly endocytotic in vivo, and endocytosis is stimulated under proteinuric conditions. (**A**–**F**) WT or *Lamb2*$^{-/-}$ mice were injected i.v. with 70 kDa FITC-Ficoll (**A**–**C**, green) or 10 kDa FITC-dextran (**D**–**F**, green). Twenty-four hours after injection, glomerular sections were stained for laminin α5 (**A**, **B**, **D**, and **E**, red) or podocin (**C** and **F**, red) and counterstained with Hoechst 33342 (blue). Insets are enlarged images of the indicated areas. (**G** and **H**) Control or Adriamycin-injected mice were injected i.v. with FITC-albumin (green). Twenty-four hours after injection, glomerular sections were stained for podocin (red) and DAPI (blue). Images are representative of at least 3 independent experiments. Original magnification, ×120 (all insets enlarged ×1.8).

to FFAs may function as a maladaptive one, leading to podocyte dysfunction and death. Loss of albumin during proteinuria and the subsequent increase of unbound FFAs have been implicated in nephrotic syndrome as an inducer of ANGPTL4 expression in podocytes (26). Our work suggests that FFAs may be involved in the development of nephrotic syndrome not only by inducing ANGPTL4, but also by directly affecting podocytes.

Results

Podocytes are highly endocytotic in vivo. Electron micrographs of the kidney often reveal intracellular vesicles in podocytes (8–14). Twenty-four hours after injection with fluorescently labeled fluid-phase tracers (70 kDa FITC-Ficoll), confocal imaging of the kidney glomerulus showed fluorescence labeling, suggesting endocytic uptake (Figure 1A). To examine fluid-phase uptake during proteinuria, we carried out similar experiments with a mouse model of nephrotic syndrome, the laminin β2-KO (*Lamb2*$^{-/-}$) mouse (27–29). The uptake of FITC-Ficoll was markedly increased in the *Lamb2*$^{-/-}$ mice and occurred in cells that were labeled with podocin, a podocyte-specific marker (Figure 1, B and C). The increased uptake in the nephrotic mice was not simply the result of more tracers crossing the disrupted GBM and reaching the podocytes; the uptake of 10 kDa FITC-dextran, which readily passes through intact as well as disrupted GBM was also increased during proteinuria (Figure 1, D–F). Increased uptake of FITC-albumin and FITC-dextran (data not shown) by podocytes also occurred in Adriamycin-treated mice, a different model of nephrotic syndrome, as compared with that observed in untreated control mice (Figure 1, G and H). These results suggested that uptake of extracellular fluid is stimulated in podocytes during proteinuria.

Albumin stimulates macropinocytosis in podocytes. To study fluid-phase endocytosis in podocytes in vitro, we incubated immortalized podocytes in culture with 70 kDa FITC-dextran. In the absence of any stimulus, moderate amounts of uptake were detected by both immunofluorescence and flow cytometry when podocytes were incubated at 37°C, but not at 4°C (Figure 2, A–C). To mimic the increased exposure to plasma proteins during proteinuria, we incubated podocytes with highly abundant plasma proteins. The addition of BSA dramatically increased the uptake of FITC-dextran (Figure 2, A–C). This effect was specific to albumin,

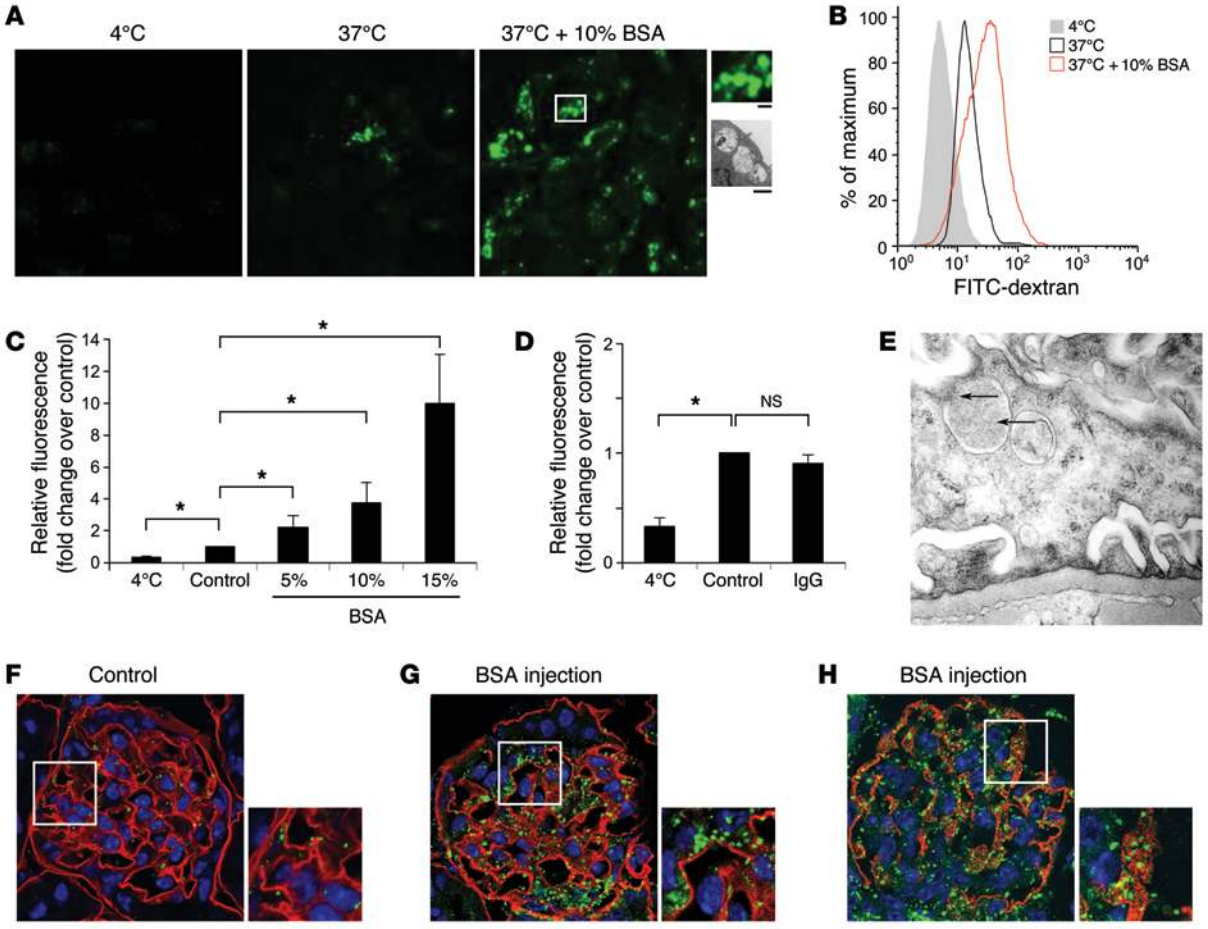

Figure 2. Albumin stimulates fluid-phase uptake in podocytes. (**A** and **B**) Cultured podocytes were incubated in the presence of 70 kDa FITC-dextran for 30 minutes and analyzed by (**A**) fluorescence microscopy or (**B**) flow cytometry. Upper inset in (**A**) is an enlarged image of the indicated area. Lower inset is an electron microscopic image of a cultured podocyte incubated with 10% BSA. In **A**, original magnification of 3 left panels, ×20; far right insets scale bars: 0.5 μm. (**C** and **D**) Podocytes were incubated with BSA or IgG in the presence of 70 kDa FITC-dextran for 30 minutes and analyzed by flow cytometry. Results are shown as the fold change in mean fluorescence intensity. Data represent the mean ± SD of 3 independent experiments analyzed by ANOVA, followed by Bonferroni's post-hoc analysis. $^*P \leq 0.05$. (**E**) The glomerulus of a mouse injected daily with BSA for 4 days was analyzed by electron microscopy. Arrows indicate protein-filled vesicles inside podocytes. (**F**–**H**) Control mice or mice given daily injections of BSA for 4 days were injected i.v. with 70 kDa FITC-Ficoll (green). Glomerular sections were stained for laminin α5 (**F** and **G**, red) or podocin (**H**, red) and counterstained with Hoechst 33342 (blue). Insets are enlarged images of the indicated areas. (**E**–**H**) Original magnification, ×120 (insets enlarged ×1.8). Images in **A** and **E**–**H** are representative of at least 3 independent experiments.

as the addition of IgG, another abundant plasma protein, did not have any effect (Figure 2D). Stimulation of endocytosis was also observed in mice injected with BSA (Figure 2, E–H).

Immunofluorescence and electron microscopy revealed that the size of the endocytosed vesicles ranged from 0.2 to 0.6 μm (Figure 2A), which suggested that the tracers were being endocytosed by macropinocytosis. Macropinocytosis is a specific process that can be distinguished from other types of fluid-phase uptake by the size of the endocytic vesicles and the ability to internalize larger molecules (30). BSA enhanced uptake of high-molecular-weight fluorescent tracers (500 kDa and 2,000 kDa) (Figure 3A). Treatment of cells with mannan to inhibit mannose receptor–mediated internalization of dextran did not affect stimulation of uptake by BSA (Figure 3A). In addition, inhibition of key components of macropinocytosis (aquaporin, PI3K, actin polymerization) blocked BSA-stimulated dextran uptake in podocytes (Figure 3B). These results indicated that the fluid-phase uptake stimulated by BSA was mediated by macropinocytosis.

To assess the level of macropinocytosis in podocytes, we compared podocytes with immature DCs, which are known to exhibit a high rate of constitutive macropinocytosis (31). While DCs showed higher levels of uptake compared with untreated podocytes, BSA induced a rate of macropinocytosis in podocytes that surpassed that of DCs (Figure 3C). Macropinocytosis in DCs was not affected by BSA, suggesting that regulation of macropinocytosis in podocytes is distinct from that in other cell types. Indeed, incubation with EGF and PDGF, which are known activators of macropinocytosis (25, 32), did not stimulate macropinocytosis in podocytes, even though downstream targets like ERK were activated (Figure 3D).

FFAs bound to albumin are the stimuli for podocyte macropinocytosis. A major function of albumin is to bind hydrophobic molecules (33). In contrast to conventional BSA, FFA-free BSA did not induce macropinocytosis (Figure 4A), while lipids isolated from BSA or clinical-grade human serum albumin (HSA) stimulated macropinocytosis (Figure 4B). This suggested that plasma lipids bound to albumin were the causative factors stimulating macropinocytosis.

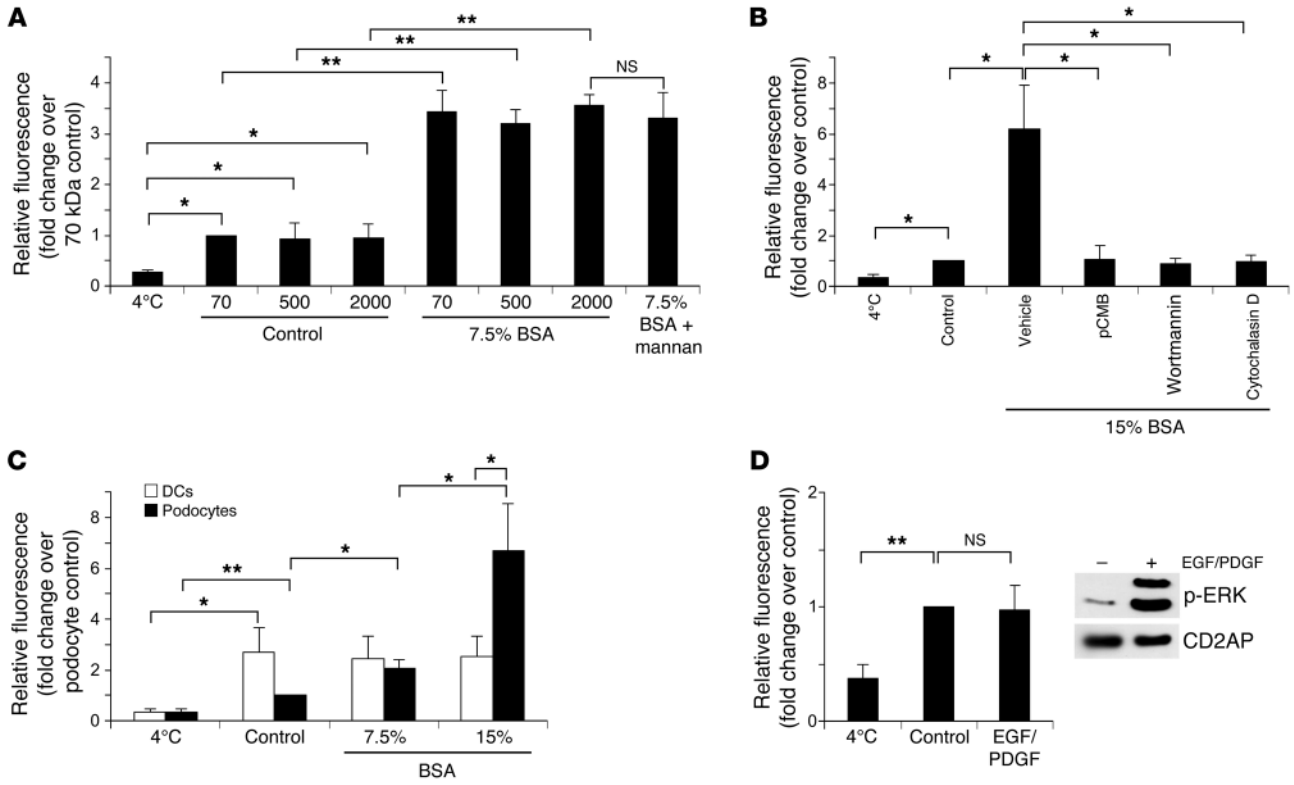

Figure 3. Albumin-stimulated fluid-phase uptake in podocytes occurs by macropinocytosis. (**A**) Podocytes were incubated with 70 kDa, 500 kDa, or 2,000 kDa FITC-dextran in the presence of 7.5% BSA and mannan (1 mg/ml) for 30 minutes and analyzed by flow cytometry. (**B**) Podocytes were pretreated with pCMB (100 μM), wortmannin (1 μM), or cytochalasin D (10 μM) for 30 minutes. The cells were subsequently incubated with 15% BSA and the inhibitors in the presence of FITC-dextran for 30 minutes and analyzed by flow cytometry. (**C**) BM-derived DCs and podocytes were incubated with BSA in the presence of FITC-dextran for 30 minutes and analyzed by flow cytometry. (**D**) Podocytes were incubated with EGF (100 nM) and PDGF (25 nM) in the presence of FITC-dextran for 30 minutes and analyzed by flow cytometry. Inset is an immunoblot of cells to detect p-ERK, with CD2AP used as a loading control, and is representative of 3 independent experiments. All results are shown as the fold change in mean fluorescence intensity. Data represent the mean ± SD of 3 independent experiments analyzed by ANOVA, followed by Bonferroni's post-hoc analysis. $^*P \le 0.05$; $^{**}P \le 0.01$.

The activity in the lipid extracts was resistant to boiling or hydrolysis in acid or base (data not shown). Incubating the lipids with hydroxylamine (cleavage of ester bonds), methanolic HCl (cleavage of ester, glycosidic, and amide bonds), or periodate (oxidation of sugar moieties) also did not significantly reduce activity (data not shown).

We tested candidate lipid molecules to identify the active lipid compound(s). Initial assays using bioactive lipids (lysophosphatidic acid, prostaglandins, lipopolysaccharide, sphingosylphosphorylcholine, etc.) or lipids with various polar head groups (choline, ethanolamine, *n*-dansyl-ethanolamine, *n*-pyrenesulfonyl-ethanolamine) did not result in stimulation of macropinocytosis (data not shown). However, several different FFAs, including oleic acid, eicosatrienoic acid (ETA), eicosapentaenoic acid (EPA), and docosahexaenoic acid (DHA) stimulated macropinocytosis in a dose-dependent manner (Figure 4C). When combined, the different FFAs had an additive effect and induced dextran uptake to levels comparable to those in BSA lipid extracts (Figure 4D). Thus, several different FFAs can stimulate macropinocytosis in podocytes.

Stimulation of macropinocytosis by albumin-associated FFAs is mediated by lipid-binding GPCRs and Gβ. Since many lipids induce their effects through specific receptors, we searched podocyte expression datasets (34) for expression of lipid receptors, focusing on GPCRs. This showed that podocytes express a variety of lipid-binding GPCRs, including FFA receptors 1, 2, and 3 (FFAR1, FFAR2, and FFAR3) (data not shown). The ligands of FFAR1 are medium- and long-chain fatty acids, whereas FFAR2 and FFAR3 bind to short-chain fatty acids. To determine their roles in podocyte macropinocytosis, we used siRNA or shRNA to knock down the expression of these receptors (Figure 5A and Supplemental Figure 1A; supplemental material available online with this article; doi:10.1172/JCI79641DS1). Lipid-induced macropinocytosis was decreased when any one of the FFAR isoforms was reduced (Figure 5B and Supplemental Figure 1B). Simultaneous knockdown of all 3 isoforms led to a further reduction (Figure 5B).

Triggering of GPCRs stimulates the disassembly and activation of heterotrimeric G proteins composed of the Gα, Gβ, and Gγ subunits. Stimulation of podocytes with lipids induced elevation of cAMP levels, a second messenger known to be regulated by GPCRs through Gα signaling (Supplemental Figure 2, A and B). However, treatment of podocytes with forskolin (an activator of adenylate cyclase) or cAMP analogs had no effect on dextran uptake (Supplemental Figure 2C). Furthermore, macropinocytosis was not induced when constitutively active $G\alpha_s$ (Q227L) was overexpressed (Supplemental Figure 2D). These results indicated that cAMP does not mediate the stimulation of macropinocytosis.

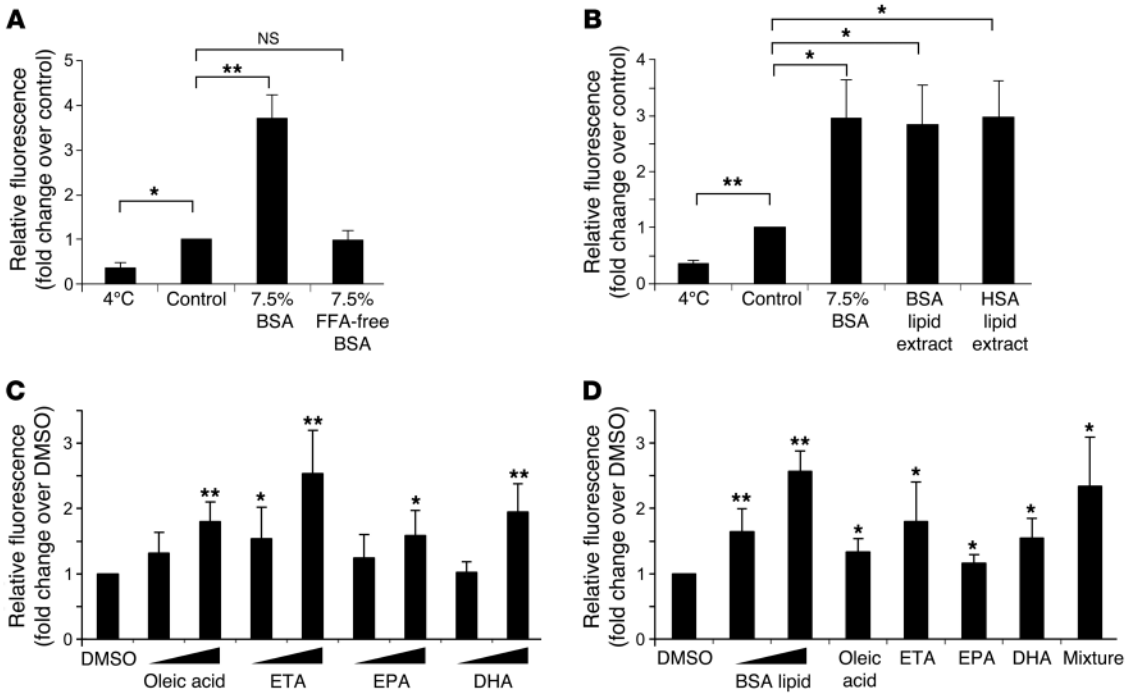

Figure 4. Podocyte macropinocytosis is stimulated by albumin-associated FFAs. (**A**) Podocytes were incubated with 7.5% BSA or FFA-free BSA in the presence of FITC-dextran for 30 minutes and analyzed by flow cytometry. (**B**) Podocytes were incubated with 7.5% BSA, BSA lipid extract, or HSA lipid extract in the presence of FITC-dextran for 30 minutes and analyzed by flow cytometry. (**C**) Podocytes were incubated with increasing concentrations (1 or 10 μM) of FFAs in the presence of FITC-dextran for 30 minutes and analyzed by flow cytometry. (**D**) Podocytes were incubated with individual FFAs (2 μM) or a mixture of the FFAs (2 μM each) in the presence of FITC-dextran for 30 minutes and analyzed by flow cytometry. All results are shown as the fold change in mean fluorescence intensity. Data represent the mean ± SD of 3 independent experiments analyzed by ANOVA, followed by Bonferroni's post-hoc analysis. *$P \leq 0.05$; **$P \leq 0.01$.

In addition to triggering the Gα subunit, GPCR signaling induces the release of the Gβ/Gγ complex, which activates its own downstream effectors, including PI3K and RAC1 (35). To determine whether the Gβ/Gγ complex mediates lipid-induced macropinocytosis, we incubated podocytes with gallein, an inhibitor of Gβ. Fluorescein, a compound similar in structure to gallein that does not inhibit Gβ, was used as a control. Gallein reduced basal and lipid-induced dextran uptake in podocytes (Figure 6A). High concentrations of gallein almost completely blocked the stimulation of micropinocytosis by lipids.

These results were confirmed using shRNA to inhibit expression of Gβ. Expression analysis showed that 2 of the 4 Gβ isoforms, Gβ1 and Gβ2, are expressed in cultured podocytes (data not shown). Immunoblotting with isoform-specific Abs showed a significant reduction of specific Gβ isoforms in *Gnb1* and *Gnb2* single-knockdown podocytes (Figure 6B and Supplemental Figure 3A). Knockdown of either *Gnb1* or *Gnb2* impaired macropinocytosis induced by lipid (Figure 6C and Supplemental Figure 3B). Knockdown was less efficient in the *Gnb1/Gnb2* double-knockdown cells, consistent with the idea that the complete absence of Gβ is toxic to the cells (Figure 6B and Supplemental Figure 4). Nonetheless, knockdown of both Gβ isoforms further reduced lipid-induced macropinocytosis (Figure 6C). This confirms that the response to lipids is mediated by Gβ/Gγ subunits.

Albumin-associated FFAs induce changes in actin structures and activate RAC1 and CDC42. Macropinosomes are formed at sites of membrane ruffling. To analyze the changes in the actin cytoskeleton induced by albumin-bound FFAs, we stained podocytes with phalloidin and analyzed them by confocal microscopy. Addition of lipids extracted from BSA led to dramatic changes in cell morphology, with formation of filopodial structures (Supplemental Figure 5A). We noted similar changes after ETA treatment (Supplemental Figure 5A).

The Rho GTPases RAC1 and CDC42 are critical regulators of the actin cytoskeleton and are key regulators of macropinocytosis. To determine whether albumin-associated lipids activate RAC1 and CDC42, podocytes were transfected with fluorescence resonance energy transfer (FRET) biosensors and analyzed using live cell imaging. Albumin-associated lipids rapidly induced activation of both RAC1 and CDC42 (Supplemental Figure 5, B and C). Confirming the role of RAC1, the addition of a RAC inhibitor attenuated macropinocytosis (Supplemental Figure 5D).

High-fat diet potentiates Adriamycin-induced proteinuria. To test the role of FFAs on podocyte function in vivo, we placed mice on a high-fat diet (HFD) to increase plasma FFA levels (Figure 7A). After 8 weeks on the diet, we did not detect significant levels of albuminuria in either control or HFD-fed mice (Figure 7B, day 0), suggesting that elevated levels of FFAs by themselves do not induce proteinuria in mice. To test whether FFAs could aggravate proteinuria, we injected mice with a low dose of Adriamycin to cause podocyte injury. Following Adriamycin administration, we noted a significantly higher urine albumin/creatinine ratio in HFD-fed mice compared with that in control mice (Figure 7B, days 4 and 7). Notably, 2 of 5 HFD-fed mice eventually went on

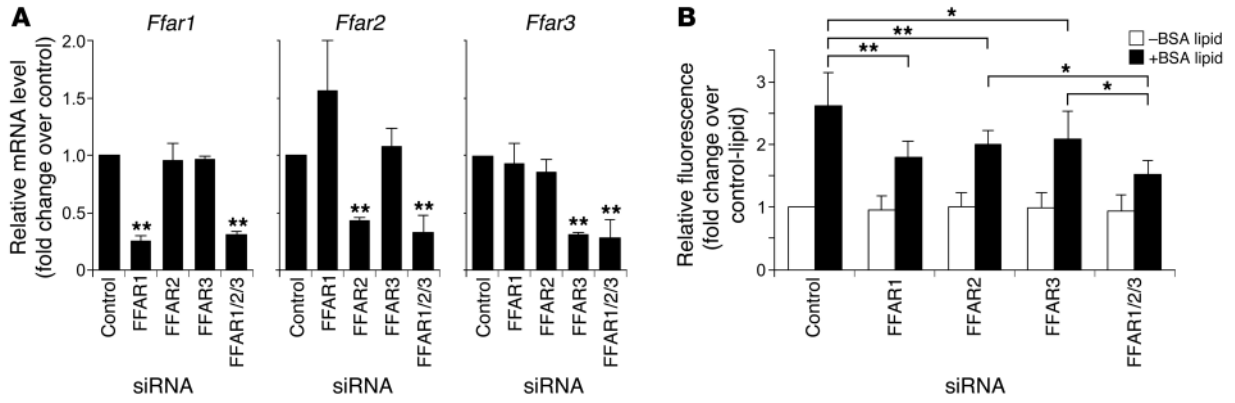

Figure 5. Stimulation of macropinocytosis by albumin-associated lipids is mediated by FFARs. (**A**) *Ffar*-knockdown podocytes were analyzed by quantitative PCR. Results are shown as the fold change of mRNA levels compared with those of controls. (**B**) Control and *Ffar*-knockdown podocytes were incubated with FITC-dextran and BSA lipid extracts for 30 minutes and analyzed by flow cytometry. Results are shown as the fold change in mean fluorescence intensity. Data represent the mean ± SD of 3 independent experiments analyzed by ANOVA, followed by Bonferroni's post-hoc analysis. $*P \leq 0.05$; $**P \leq 0.01$.

to develop severe proteinuria (Figure 7B, day 24) compared with none of the control mice. These results suggest that high FFA levels can aggravate podocyte injury and exacerbate proteinuria.

Discussion

Large vesicles within podocytes are often seen by electron microscopy in proteinuric kidney diseases (7). There has been much speculation about the origin of these vesicles (36–39), but their functional significance has remained unresolved. Recent studies have demonstrated that impairment of the endocytic machinery in podocytes leads to proteinuria, indicating that endocytosis may play a crucial role in podocyte function (19, 40, 41). Our results reveal that podocytes induce significant levels of macropinocytosis in response to FFAs. FFAs stimulate macropinocytosis through a pathway distinct from that in other cell types, one that involves FFARs, Gβ/Gγ, and RAC1.

Our results indicate that podocytes are capable of internalizing large amounts of extracellular fluid and molecules by macropinocytosis. Demonstrating whether fluid-phase uptake occurs by macropinocytosis is not a straightforward task because of the nonspecific nature of its cargo and the lack of signature marker proteins. The uptake of large molecules is considered the most reliable measure of macropinocytosis. Tracer molecules larger than 70 kDa are internalized predominantly by macropinocytosis, since the small size of micropinosomes or endosomes restricts both the size and numbers of high molecular weight molecules (42). We showed that podocytes were able to efficiently internalize 70 kDa dextran in vivo (Figure 1, A–C) and even larger dextrans (up to 2,000 kDa) in vitro (Figure 3A), consistent with macropinocytosis. Suppression of uptake by inhibitors of PI3K, aquaporin, and actin polymerization further lends support for macropinocytosis as the phenomenon we measured (Figure 3B).

The role of macropinocytosis varies depending on cell type. Immature DCs use macropinocytosis as a means of surveying the surrounding environment for foreign pathogens (23). In *Dictyostelium* and Ras-transformed cells, macropinocytosis serves as a major pathway for nutrient supply (43, 44). In some conditions, macropinocytosis is transiently induced by certain stimuli such as phorbol esters or growth factors such as EGF or CSF-1 (25, 32, 45).

Our work suggests that macropinocytosis may be involved in the removal of plasma proteins that enter and cross the GBM. Because the filter is not completely effective, it has been argued that an active clearance mechanism must exist to prevent the filter from clogging. The high expression of receptors for albumin, IgG, and complement on podocytes support the idea that podocytes play a specialized role in the uptake and removal of plasma proteins that cross the GBM.

Macropinocytosis may also be a route of nutrient uptake in podocytes, similar to Ras-transformed cells (43, 44). Podocytes are unique in that they are located wholly in the urinary space and are separated from the blood supply by the GBM. This might restrict their exposure to nutrients, partially explaining why podocytes exhibit constitutive autophagy and why impairing autophagy is detrimental to podocytes (46, 47). We observed trafficking of the macropinosomes to the lysosomes in podocytes (data not shown), and it is therefore plausible to speculate that proteins internalized via macropinocytosis can be degraded and used as a source of energy and anabolic substrates.

It is interesting that FFAs can induce macropinocytosis. FFAs have been implicated in a feedback loop that mediates the hypertriglyceridemia that accompanies nephrotic syndrome (26). Significant urinary loss of albumin decreases the plasma lipid–buffering capacity, leading to elevated levels of unbound FFAs (26). It was recently shown that this elevation of FFAs increases circulating ANGPTL4, which inhibits lipoprotein lipase, and thereby leads to elevated plasma triglycerides (26). Notably, ANGPTL4 produced from podocytes induces proteinuria in rats through mechanisms that are yet to be elucidated (26, 48). We found that FFAs induced ANGPTL4 expression in podocytes (Supplemental Figure 6), indicating that FFAs could induce proteinuria through ANGPTL4 induction.

Our findings, however, also suggest that FFAs could affect proteinuria by directly altering podocyte function and viability. We and others have previously shown that RAC1 activation in podocytes leads to podocyte foot process effacement and proteinuria in mice (49, 50). In addition, excessive macropinocytosis and accumulation of albumin in podocytes has been shown to induce lysosomal dysfunction, podocyte loss, and subsequent glomerulo-

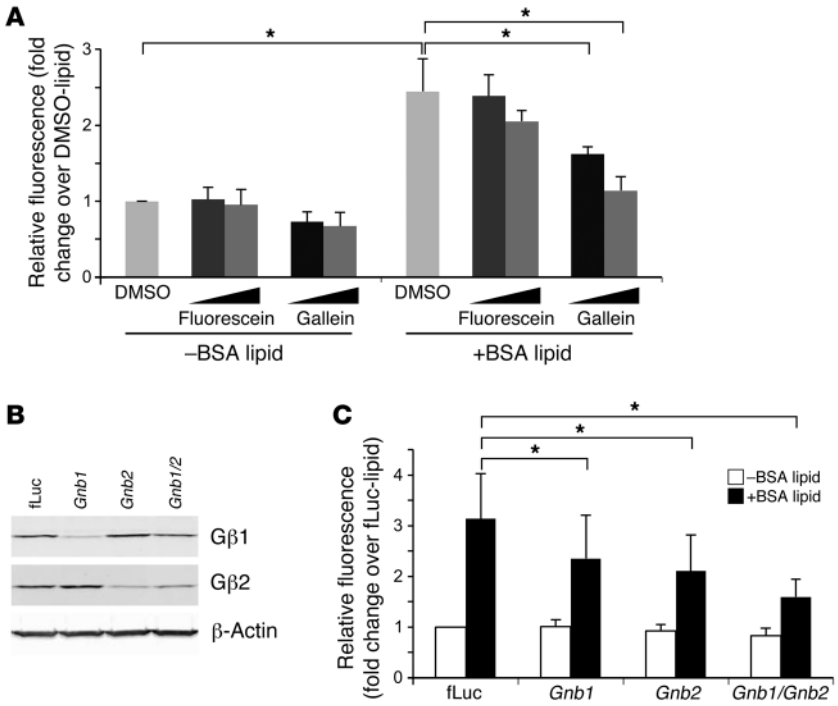

Figure 6. Stimulation of macropinocytosis by albumin-associated lipids is mediated by Gβ activation. (**A**) Podocytes were pretreated with 2 or 10 μM fluorescein or gallein for 30 minutes. Subsequently, the cells were incubated with BSA lipid extract in the presence of rhodamine B–dextran for 30 minutes and analyzed by flow cytometry. (**B**) Podocytes expressing shRNAs targeting firefly luciferase (fLuc), *Gnb1*, *Gnb2*, or *Gnb1* and *Gnb2* (*Gnb1/2*) were immunoblotted for Gβ1 and Gβ2 expression. β-Actin was used as a loading control. A representative blot of 3 independent experiments is shown. (**C**) GNB-knockdown podocytes were incubated with BSA lipid extracts in the presence of rhodamine B–dextran for 30 minutes and analyzed by flow cytometry. Results in **A** and **C** are shown as the fold change in mean fluorescence intensity. Data represent the mean ± SD of 3 independent experiments analyzed by ANOVA, followed by Bonferroni's post-hoc analysis. $^*P \leq 0.05$

sclerosis (15, 16, 51–55). Consistent with this, we found that mice with elevated FFA levels were more susceptible to Adriamycin and exhibited significantly higher levels of albuminuria (Figure 7). The effects of a HFD on the kidney are complex, and there may be additional factors that are affecting proteinuria, but the results are consistent with a role for FFAs.

It is intriguing to consider the possibility that an interplay between FFAs and ANGPTL4 plays a critical role in the transition from proteinuria to full-blown nephrotic syndrome. Podocyte injury would lead to proteinuria, but the transition to nephrotic syndrome might involve the elevation of both plasma FFAs and ANGPTL4. The combined effect of albuminuria and hyperlipidemia (caused by elevated ANGPTL4) would lead to an increase in the FFA/albumin ratio. Once the level of FFAs exceeds the buffering capacity of albumin, the FFAs could play a key role in a vicious cycle of persistent albuminuria and podocyte damage that converts proteinuria into nephrotic syndrome. In support of this idea, lipoprotein apheresis to lower lipid levels reduces proteinuria and improves renal function in some patients with nephrotic syndrome (56). While it is unclear whether elevated plasma FFAs are sufficient by themselves to initiate proteinuria, our work suggests that once proteinuria has begun, FFAs can amplify the consequences of proteinuria.

Taken together, we have identified a pathway of inducible macropinocytosis in podocytes that may play a role in maintenance of the glomerular filtration barrier. Persistent activation of this pathway during proteinuria, however, may have maladaptive consequences and lead to nephrotic syndrome. FFAs and FFARs are new potential targets for the treatment of nephrotic syndrome.

Methods

Reagents. FITC-Ficoll (70 kDa), FITC-dextran (10, 70, 150, 500, 2,000 kDa), Adriamycin, BSA, mouse serum IgG, mannan, *p*-chloromercuriobenzoate (*p*CMB), wortmannin, cytochalasin D, recombinant EGF, ovalbumin, 8-Br-cAMP, 8-pCPT-2′-O-Me-cAMP, forskolin, 3-isobutyl-1-methylxanthine (IBMX), isoproterenol, fluorescein, anti-podocin Ab (catalog P0372), and anti–β-actin Ab (clone AC-15) were obtained from Sigma-Aldrich. FFA-free BSA was purchased from SeraCare Life Sciences. HSA was purchased from Williams Medical Company. Hoechst 33342 and recombinant PDGF was purchased from Life Technologies. Anti–phospho-ERK Ab (clone 197G2) was obtained from Cell Signaling Technology. Rhodamine B-dextran (70 kDa) was purchased from Nanocs. Oleic acid, eicosatetraenoic acid, eicosapentaenoic acid, and docosahexaenoic acid were obtained from Nu-Chek Prep. Gallein and EHT1864 was purchased from Tocris Bioscience. Anti-Gβ1 (catalog sc-379) and anti-Gβ2 (catalog sc-380) antibodies were purchased from Santa Cruz Biotechnology Inc. Anti–laminin α5 (57) and anti-CD2AP (58) Abs have been previously described.

Mice. All mice were housed in a specific pathogen–free facility at Washington University School of Medicine. C57BL/6J, 129/SvJ, and BALB/cJ mice were obtained from The Jackson Laboratory. Laminin β2–knockout (*Lamb2*$^{-/-}$) mice with a muscle-specific rescue transgene have been described previously (27–29). For HFD experiments, age- and weight-matched male 129/SvJ mice were randomly grouped and given a normal chow diet (13 kcal% fat; LabDiet) or a HFD (60 kcal% fat, D12492; Research Diets Inc.). After 8 weeks on the diet, mice were injected i.v. with Adriamycin (10 mg/kg body weight) or an equal volume of saline as a control.

Cell culture. Conditionally immortalized podocytes were generated as described previously (59) and maintained at 33°C in RPMI1640 supplemented with 10% FBS, 1 mM sodium pyruvate, 10 mM HEPES, 100 U/ml penicillin, 100 μg/ml streptomycin, 0.1 mM β-mercaptoethanol, and 100 U/ml recombinant mouse IFN-γ (a gift of Robert Schreiber, Washington University, St. Louis, Missouri, USA).

BM-derived DCs were cultured as previously described (60). Briefly, BM cells were cultured in Iscove's modified Dulbecco's medium (IMDM) supplemented with 10% FBS (Hyclone), 1 mM

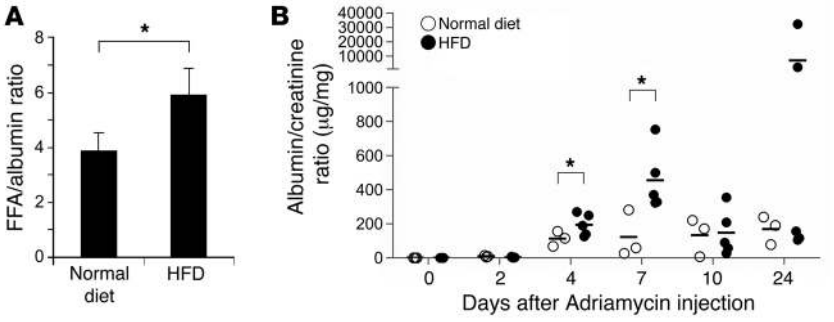

Figure 7. Mice fed a HFD are more susceptible to Adriamycin-induced proteinuria. Mice were given either a normal diet or a HFD. (**A**) After 8 weeks, serum was collected and analyzed by ELISA for FFA and albumin concentrations. (**B**) Mice were then given a single i.v. injection of Adriamycin (10 mg/kg). Urine was collected periodically after injection and analyzed for albumin/creatinine ratios. $n = 3$, normal diet; $n = 5$, HFD. Samples were compared using the Student's *t* test (**A**) or ANOVA, followed by Bonferroni's post-hoc analysis (**B**). $^*P \leq 0.05$.

sodium pyruvate, 10 mM HEPES, 100 U/ml penicillin, 100 μg/ml streptomycin, 0.1 mM β-mercaptoethanol, and 100 ng/ml recombinant granulocyte macrophage colony-stimulating factor (rGM-CSF) (R&D Systems) for 8 days.

Electron microscopy. Slices of kidney cortex or podocytes cultured on coverslips were fixed overnight in 4% paraformaldehyde (PFA) and 4% glutaraldehyde in 0.1 M sodium cacodylate buffer followed by repeated washes in PBS. After postfixation in 1% osmium tetraoxide, the samples were reduced with 1.5% potassium ferrocyanide for 1 hour at 4°C. Subsequently, the samples were washed, dehydrated in graded alcohol, and embedded in resin according to standard protocols.

In vivo endocytosis. WT or *Lamb2*$^{-/-}$ mice were injected i.v. with a bolus of FITC-Ficoll (70 kDa) or FITC-dextran (10 kDa) in 0.9% NaCl at a dose of 250 mg/kg of body weight. BALB/cJ mice were injected i.v. with Adriamycin (10 mg/kg body weight) or an equal volume of saline as a control. Six days after the Adriamycin injection, the mice were injected i.v. with FITC-labeled albumin (250 mg/kg body weight). For BSA injection experiments, mice (C57BL/6J and 129/SvJ mixed background) were given a daily i.p. injection of endotoxin-free BSA (15 mg/g body weight in PBS) for 4 days. On day 4, the mice were injected i.v. with 70 kDa FITC-dextran (250 mg/kg body weight). Twenty-four hours after injection of FITC-labeled tracers, kidneys were harvested from mice, embedded in OCT (VWR International), and snap-frozen in methylbutane cooled in a dry ice ethanol bath. Cryosections (8 μm) were applied to charged slides using a cryostat.

For immunofluorescence assays, the kidney sections were fixed with 1% PFA in PBS for 5 minutes, followed by blocking and permeabilization with 2% FBS in PBS with 0.1% saponin. The slides were incubated with Abs against laminin α5 or podocin for 1 hour at room temperature, followed by extensive washing. Fluorescently conjugated secondary Abs were then applied for 1 hour at room temperature. After several washes, the slides were imaged on an Olympus FV1000 confocal microscope.

In vitro macropinocytosis assays. Mouse podocytes in 6-well plates were serum starved with serum-free RPMI for 2 hours. The cells were then incubated in RPMI supplemented with 0.5 mg/ml FITC- or rhodamine B–dextran for 30 minutes on ice or at 37°C. The cells were subsequently washed 3 times with ice-cold PBS and fixed with 4%PFA for confocal microscopic analysis or trypsinized and resuspended in FACS buffer (2% FBS and 2 mM EDTA in 1× PBS) for flow cytometric analysis. FACS data were collected on FACSCanto II or LSR II flow cytometers (BD Biosciences) and analyzed with FlowJo software.

Western blots. Podocytes were lysed in a modified radioimmunoprecipitation assay (RIPA) lysis buffer (50 mM Tris-HCl [pH 7.4], 150 mM NaCl, 1 mM EDTA, 1% NP-40, 0.25% sodium deoxycholate, 1 mM PMSF, 1 μg/ml aprotinin, 1 μg/ml leupeptin, 1 μg/ml pepstatin, 1 mM Na_3VO_4, 1 mM NaF) for 30 minutes on ice. The protein content of the lysates was quantified with a protein assay kit (Bio-Rad). Equivalent amounts of each sample were separated by SDS-PAGE, transferred to nitrocellulose membranes, and immunoblotted for phosphorylated ERK (p-ERK), CD2AP, Gβ1, Gβ2, or β-actin. The blots were visualized by ECL or infrared imaging on a LI-COR Odyssey system (LI-COR).

Lipid extraction. Lipids were extracted from BSA or HSA using the Bligh-Dyer method with minor modifications. Three milliliters of 20% BSA in ddH_2O was added to a mixture of 6 ml chloroform and 12 ml methanol in a glass tube and mixed on an orbital shaker for 15 minutes at room temperature. Chloroform (6 ml) was added to the mixture while vortexing at low speeds, followed by 6 ml of 1 M NaCl. The samples were centrifuged at 800 *g* for 5 minutes to separate the aqueous and organic phases. The lower organic phase was carefully collected, aliquoted into 1-ml tubes, evaporated under vacuum, and stored at –80°C.

For endocytosis assays, the lipids were resuspended in 30 μl DMSO, and the cells were treated with 1 to 5 μl/ml lipid suspension. Assuming loss of 50% of the lipids during extraction, this is estimated to be equivalent to the amount of lipids bound to BSA in a 0.066% to 0.33% solution.

Gene knockdown and overexpression experiments. ON-TARGETplus siRNA targeting FFAR isoforms was purchased from Dharmacon (GE Healthcare). Podocytes were transfected with a pool of siRNAs containing 4 individual siRNAs targeting each isoform using the Nucleofector System (Lonza). Transfection efficiency was monitored using the siGLO Green Transfection Indicator (GE Healthcare).

Lentiviral constructs containing shRNAs targeting FFAR isoforms, Gβ isoforms, and firefly luciferase (control) were generated using the pFLRu-YFP lentiviral vector (61). The targeting sequences were: fLuc, CCAACCCTATTCTCCTTCT; FFAR1, ATCTTTGCCTTGGCCCACTTTG; FFAR2, CGGTTTGCTACTGATCCGCAAT; FFAR3, ACTGGAACTGAAGGTAAAGAAT; GNB1, CATTATCTGTGGTAT CACA; GNB2, CATCTGCTCCATCTATAGT. PCR products containing the *U6* promoter followed by the shRNA sequences were cloned into the pFLRu-YFP vector using the *XbaI*/*XhoI* site.

For lentivirus production, 293T cells were transfected with the lentiviral constructs along with packaging plasmids (pMDLg/pRRE and pRSV-Rev) and an envelope plasmid (pMD2.G). Proliferating podocytes were infected with supernatants containing lentivirus and 8 μg/ml protamine sulfate for 24 hours. Cells expressing high levels of YFP were sorted on a FACSAria II flow cytometer (BD Biosciences) 7 days after infection.

To generate podocytes stably expressing constitutively active Gαs, cells were transfected with a pcDNA3.1 vector containing $G\alpha_s$ (Q227L) (a gift of Kun-Liang Guan, UCSD, San Diego, California, USA). Sta-

bly transfected cells were selected by serial passage in 400 μg/ml G418 for 1 week.

cAMP FRET assays. A pcDNA3 plasmid containing the FRET-based cAMP biosensor $^{T}Epac^{vv}$ was a gift of Kees Jalink (The Netherlands Cancer Institute, Amsterdam, The Netherlands). Cultured podocytes were transfected with $^{T}Epac^{vv}$ using the Nucleofector System and seeded on glass-bottom dishes (MatTek Corp.). Images were obtained using an Olympus FV1000 confocal microscope in a temperature-controlled chamber (37°C). The cells were excited at 440 nm, and donor and acceptor emission was detected simultaneously using a 510 nm beamsplitter and 2 photomultipliers with optical filters: 465–495 nm (CFP) and 535 to 565 nm (YFP).

FRET measurements were quantified using ImageJ software (NIH) and the Ratio Plus plugin. After regions were drawn around individual cells, emission ratios were obtained by calculating FRET intensities divided by donor intensities. Time-course ratio measurements were normalized to baseline values before stimulation. The FRET value was set at 1 at the onset of the experiment.

FFA, albumin, and creatinine assays. Mouse serum and urine samples were collected at the indicated time points. FFA (BioVision), albumin (Bethyl Laboratories Inc.), and creatinine (BioAssay Systems) levels were quantified by ELISA according to the manufacturers' instructions.

Statistics. Data are presented as the mean ± SD. We determined significance by ANOVA or a 2-tailed Student's *t* test as indicated in the figure legends. ANOVA, followed by Bonferroni's post-hoc analysis, was used to determine significant differences in experiments with 3 or more samples. A *P* value of 0.05 or less was considered statistically significant.

Study approval. Animal care and experiments were conducted in accordance with protocols approved by the Animal Studies Committee of Washington University (protocol number 20120013), in compliance with the Animal Welfare Act.

Acknowledgments

This research was supported by the Howard Hughes Medical Institute; NIH grants R01DK058366 (to A.S. Shaw) and RO1HL118639 (to R.W. Gross); the German Research Foundation (CRC 992 and CRC 1140, Heisenberg-Professorship, to T.B. Huber); the European Research Council; and the Excellence Initiative of the German Federal and State Governments (EXC 294, to T.B. Huber).

Address correspondence to: Andrey Shaw, Department of Pathology and Immunology, Box 8118, Washington University School of Medicine, 660 South Euclid, Saint Louis, Missouri 63110, USA. Phone: 314.362.4614; E-mail: ashaw@wustl.edu.

1. Haraldsson B, Nystrom J, Deen WM. Properties of the glomerular barrier and mechanisms of proteinuria. *Physiol Rev*. 2008;88(2):451–487.
2. Edwards A, Daniels BS, Deen WM. Ultrastructural model for size selectivity in glomerular filtration. *Am J Physiol*. 1999;276(6):F892–F902.
3. Lazzara MJ, Deen WM. Effects of plasma proteins on sieving of tracer macromolecules in glomerular basement membrane. *Am J Physiol Renal Physiol*. 2001;281(5):F860–F868.
4. Deen WM, Lazzara MJ, Myers BD. Structural determinants of glomerular permeability. *Am J Physiol Renal Physiol*. 2001;281(4):F579–F596.
5. Smithies O. Why the kidney glomerulus does not clog: a gel permeation/diffusion hypothesis of renal function. *Proc Natl Acad Sci U S A*. 2003;100(7):4108–4113.
6. Farquhar MG, Vernier RL, Good RA. Studies on familial nephrosis. II. Glomerular changes observed with the electron microscope. *Am J Pathol*. 1957;33(4):791–817.
7. Farquhar MG, Vernier RL, Good RA. An electron microscope study of the glomerulus in nephrosis, glomerulonephritis, and lupus erythematosus. *J Exp Med*. 1957;106(5):649–660.
8. Caulfield JP, Farquhar MG. The permeability of glomerular capillaries to graded dextrans. Identification of the basement membrane as the primary filtration barrier. *J Cell Biol*. 1974;63(3):883–903.
9. Venkatachalam MA, Cotran RS, Karnovsky MJ. An ultrastructural study of glomerular permeability in aminonucleoside nephrosis using catalase as a tracer protein. *J Exp Med*. 1970;132(6):1168–1180.
10. Venkatachalam MA, Karnovsky MJ, Fahimi HD, Cotran RS. An ultrastructural study of glomerular permeability using catalase and peroxidase as tracer proteins. *J Exp Med*. 1970;132(6):1153–1167.
11. Vogt A, Bockhorn H, Kozima K, Sasaki M. Electron microscopic localization of the nephrotoxic antibody in the glomeruli of the rat after intravenous application of purified nephritogenic antibody-ferritin conjugates. *J Exp Med*. 1968;127(5):867–878.
12. Farquhar MG, Palade GE. Glomerular permeability. II. Ferritin transfer across the glomerular capillary wall in nephrotic rats. *J Exp Med*. 1961;114:699–716.
13. Farquhar MG, Wissig SL, Palade GE. Glomerular permeability. I. Ferritin transfer across the normal glomerular capillary wall. *J Exp Med*. 1961;113:47–66.
14. Farquhar MG, Palade GE. Segregation of ferritin in glomerular protein absorption droplets. *J Biophys Biochem Cytol*. 1960;7:297–304.
15. Yoshikawa N, Ito H, Akamatsu R, Hazikano H, Okada S, Matsuo T. Glomerular podocyte vacuolation in focal segmental glomerulosclerosis. *Arch Pathol Lab Med*. 1986;110(5):394–398.
16. Abbate M, et al. Transforming growth factor-beta1 is up-regulated by podocytes in response to excess intraglomerular passage of proteins: a central pathway in progressive glomerulosclerosis. *Am J Pathol*. 2002;161(6):2179–2193.
17. Tojo A, et al. Glomerular albumin filtration through podocyte cell body in puromycin aminonucleoside nephrotic rat. *Med Mol Morphol*. 2008;41(2):92–98.
18. Kinugasa S, et al. Selective albuminuria via podocyte albumin transport in puromycin nephrotic rats is attenuated by an inhibitor of NADPH oxidase. *Kidney Int*. 2011;80(12):1328–1338.
19. Akilesh S, et al. Podocytes use FcRn to clear IgG from the glomerular basement membrane. *Proc Natl Acad Sci U S A*. 2008;105(3):967–972.
20. Doherty GJ, McMahon HT. Mechanisms of endocytosis. *Annu Rev Biochem*. 2009;78:857–902.
21. Damke H, Baba T, van der Bliek AM, Schmid SL. Clathrin-independent pinocytosis is induced in cells overexpressing a temperature-sensitive mutant of dynamin. *J Cell Biol*. 1995;131(1):69–80.
22. Kerr MC, Teasdale RD. Defining macropinocytosis. *Traffic*. 2009;10(4):364–371.
23. Sallusto F, Cella M, Danieli C, Lanzavecchia A. Dendritic cells use macropinocytosis and the mannose receptor to concentrate macromolecules in the major histocompatibility complex class II compartment: downregulation by cytokines and bacterial products. *J Exp Med*. 1995;182(2):389–400.
24. Norbury CC, Hewlett LJ, Prescott AR, Shastri N, Watts C. Class I MHC presentation of exogenous soluble antigen via macropinocytosis in bone marrow macrophages. *Immunity*. 1995;3(6):783–791.
25. Haigler HT, McKanna JA, Cohen S. Rapid stimulation of pinocytosis in human carcinoma cells A-431 by epidermal growth factor. *J Cell Biol*. 1979;83(1):82–90.
26. Clement LC, Mace C, Avila-Casado C, Joles JA, Kersten S, Chugh SS. Circulating angiopoietin-like 4 links proteinuria with hypertriglyceridemia in nephrotic syndrome. *Nat Med*. 2014;20(1):37–46.
27. Noakes PG, Miner JH, Gautam M, Cunningham JM, Sanes JR, Merlie JP. The renal glomerulus of mice lacking s-laminin/laminin [beta]2: nephrosis despite molecular compensation by laminin [beta]1. *Nat Genet*. 1995;10(4):400.
28. Miner JH, Go G, Cunningham J, Patton BL, Jarad G. Transgenic isolation of skeletal muscle and kidney defects in laminin {beta}2 mutant mice: implications for Pierson syndrome. *Development*. 2006;133(5):967–975.
29. Jarad G, Cunningham J, Shaw AS, Miner JH. Proteinuria precedes podocyte abnormalities in $Lamb2^{-/-}$ mice, implicating the glomerular basement membrane as an albumin barrier. *J Clin Invest*. 2006;116(8):2272–2279.
30. Lim JP, Gleeson PA. Macropinocytosis: an endocytic pathway for internalising large gulps. *Immu-*

nol Cell Biol. 2011;89(8):836–843.
31. Norbury CC. Drinking a lot is good for dendritic cells. *Immunology*. 2006;117(4):443–451.
32. Racoosin EL, Swanson JA. Macrophage colony-stimulating factor (rM-CSF) stimulates pinocytosis in bone marrow-derived macrophages. *J Exp Med*. 1989;170(5):1635–1648.
33. van der Vusse GJ. Albumin as fatty acid transporter. *Drug Metab Pharmacokinet*. 2009;24(4):300–307.
34. Akilesh S, et al. Arhgap24 inactivates Rac1 in mouse podocytes, and a mutant form is associated with familial focal segmental glomerulosclerosis. *J Clin Invest*. 2011;121(10):4127–4137.
35. Khan SM, et al. The expanding roles of Gbeta-gamma subunits in G protein-coupled receptor signaling and drug action. *Pharmacol Rev*. 2013;65(2):545–577.
36. Feldman JD, Fisher ER. Renal lesions of aminonucleoside nephrosis as revealed by electron microscopy. *Lab Invest*. 1959;8(2):371–385.
37. Venkatachalam MA, Karnovsky MJ, Cotran RS. Glomerular permeability. Ultrastructural studies in experimental nephrosis using horseradish peroxidase as a tracer. *J Exp Med*. 1969;130(2):381–399.
38. Rantala I. Glomerular epithelial cell endocytosis of immune deposits in the nephrotic rat. An ultrastructural immunoperoxidase study. *Nephron*. 1981;29(5):239–244.
39. Sharon Z, Schwartz MM, Pauli BU, Lewis EJ. Kinetics of glomerular visceral epithelial cell phagocytosis. *Kidney Int*. 1978;14(5):526–529.
40. Kim JM, et al. CD2-associated protein haploinsufficiency is linked to glomerular disease susceptibility. *Science*. 2003;300(5623):1298–1300.
41. Soda K, et al. Role of dynamin, synaptojanin, and endophilin in podocyte foot processes. *J Clin Invest*. 2012;122(12):4401–4411.
42. Li L, Wan T, Wan M, Liu B, Cheng R, Zhang R. The effect of the size of fluorescent dextran on its endocytic pathway [published online ahead of print January 9, 2015]. *Cell Biol Int*. doi:10.1002/cbin.10424.
43. Hacker U, Albrecht R, Maniak M. Fluid-phase uptake by macropinocytosis in Dictyostelium. *J Cell Sci*. 1997;110(pt 2):105–112.
44. Commisso C, et al. Macropinocytosis of protein is an amino acid supply route in Ras-transformed cells. *Nature*. 2013;497(7451):633–637.
45. Swanson JA. Phorbol esters stimulate macropinocytosis and solute flow through macrophages. *J Cell Sci*. 1989;94(pt 1):135–142.
46. Mizushima N, Yamamoto A, Matsui M, Yoshimori T, Ohsumi Y. In vivo analysis of autophagy in response to nutrient starvation using transgenic mice expressing a fluorescent autophagosome marker. *Mol Biol Cell*. 2004;15(3):1101–1111.
47. Hartleben B, et al. Autophagy influences glomerular disease susceptibility and maintains podocyte homeostasis in aging mice. *J Clin Invest*. 2010;120(4):1084–1096.
48. Clement LC, et al. Podocyte-secreted angiopoietin-like-4 mediates proteinuria in glucocorticoid-sensitive nephrotic syndrome. *Nat Med*. 2011;17(1):117–122.
49. Yu H, et al. Rac1 activation in podocytes induces rapid foot process effacement and proteinuria. *Mol Cell Biol*. 2013;33(23):4755–4764.
50. Babelova A, et al. Activation of Rac-1 and RhoA contributes to podocyte injury in chronic kidney disease. *PLoS One*. 2013;8(11):e80328.
51. Okamura K, et al. Endocytosis of albumin by podocytes elicits an inflammatory response and induces apoptotic cell death. *PLoS One*. 2013;8(1):e54817.
52. Chen J, Chen MX, Fogo AB, Harris RC, Chen JK. mVps34 deletion in podocytes causes glomerulosclerosis by disrupting intracellular vesicle trafficking. *J Am Soc Nephrol*. 2013;24(2):198–207.
53. Overmeyer JH, Kaul A, Johnson EE, Maltese WA. Active ras triggers death in glioblastoma cells through hyperstimulation of macropinocytosis. *Mol Cancer Res*. 2008;6(6):965–977.
54. Li C, Macdonald JI, Hryciw T, Meakin SO. Nerve growth factor activation of the TrkA receptor induces cell death, by macropinocytosis, in medulloblastoma Daoy cells. *J Neurochem*. 2010;112(4):882–899.
55. Nara A, Aki T, Funakoshi T, Unuma K, Uemura K. Hyperstimulation of macropinocytosis leads to lysosomal dysfunction during exposure to methamphetamine in SH-SY5Y cells. *Brain Res*. 2012;1466:1–14.
56. Yokoyama H, Wada T, Zhang W, Yamaya H, Asaka M. Advances in apheresis therapy for glomerular diseases. *Clin Exp Nephrol*. 2007;11(2):122–127.
57. Miner JH, et al. The laminin alpha chains: expression, developmental transitions, and chromosomal locations of alpha1-5, identification of heterotrimeric laminins 8-11, and cloning of a novel alpha3 isoform. *J Cell Biol*. 1997;137(3):685–701.
58. Dustin ML, et al. A novel adaptor protein orchestrates receptor patterning and cytoskeletal polarity in T-cell contacts. *Cell*. 1998;94(5):667–677.
59. Mundel P, et al. Rearrangements of the cytoskeleton and cell contacts induce process formation during differentiation of conditionally immortalized mouse podocyte cell lines. *Exp Cell Res*. 1997;236(1):248–258.
60. Lutz MB, et al. An advanced culture method for generating large quantities of highly pure dendritic cells from mouse bone marrow. *J Immunol Methods*. 1999;223(1):77–92.
61. Feng Y, et al. A multifunctional lentiviral-based gene knockdown with concurrent rescue that controls for off-target effects of RNAi. *Genomics Proteomics Bioinformatics*. 2010;8(4):238–245.